Spectroscopy of near-stoichiometric $LiNbO_3$:MgO,Cr crystals under high pressure

A. Kamińska
Institute of Physics, Polish Academy of Sciences, Aleja Lotników 32/46, 02-668 Warsaw, Poland

A. Suchocki
Institute of Physics, Polish Academy of Sciences, Aleja Lotników 32/46, 02-668 Warsaw, Poland
and Depertamento de Fisica de Materiales, Universidad Autonoma de Madrid, Cantoblanco, 28049 Madrid, Spain

L. Arizmendi, D. Callejo, and F. Jaque
Depertamento de Fisica de Materiales, Universidad Autonoma de Madrid, Cantoblanco, 28049 Madrid, Spain

M. Grinberg
Institute of Experimental Physics, Gdańsk University, ulica Wita Stwosza 57, 80-952 Gdańsk, Poland
(Received 2 March 2000)

The results of high-pressure spectroscopic studies of near-stoichiometric $LiNbO_3$:Cr(0.1%) and $LiNbO_3$:MgO,Cr(0.1%) crystals are reported. Much lower inhomogeneous broadening of electronic transitions in near-stoichiometric crystals than in congruent ones allows us to obtain better resolution of the spectroscopic measurements. The results of measurements show that Cr^{3+} ions occupy mostly the same centers in near-stoichiometric crystals and in the congruent ones. In near-stoichiometric crystals doped only with chromium, the Cr^{3+} ions substitute the Li^+ sites in the $LiNbO_3$ host forming one major center (denoted as center γ) and two lower concentration centers, denoted by α and β. In near-stoichiometric crystals doped additionally with a proper amount of MgO, the additional low-strength crystal-field center δ dominates the spectrum. This center corresponds to the Cr^{3+} ions in Nb^{5+} sites. The hydrostatic pressure above 75 kbar transforms this center into the high-strength crystal-field center. Due to better resolution of measurements, it was possible to determine the splitting of the ^2E level for the δ center, which is equal to about 17 cm^{-1}. Estimated values of the energy difference between the position of the $^4T_2$ and the ^2E levels for centers β, γ, and δ in these near-stoichiometric $LiNbO_3$ crystals are equal to -20, -242, and more than -1000 cm^{-1}, respectively.

I. INTRODUCTION

Cr^{3+} ions in lithium niobate crystals are known to occupy different sites in the crystal host and to produce several luminescence centers. Occupancy of various sites and centers depends on concentration of chromium dopant, stoichiometry of the host, and codoping with optically neutral ions, such as Mg or Zn. Studies of the nature of various Cr^{3+} centers in lithium niobate have a long history.[1] Optical spectroscopic methods have been applied first to establish the nature of various Cr^{3+} centers. The relatively low-strength crystal field that most of the Cr^{3+} ions experience in the $LiNbO_3$ host results in a large contribution of broadband emission to the luminescence spectra. This broadband luminescence is related to the $^4T_2 \rightarrow {}^4A_2$ optical transitions in the Cr^{3+} ion since in low crystal field the $^4T_2$ state is the first excited state. Identification of various Cr^{3+} centers is very often based in the literature on the analysis of the sharp R lines, related to the $^2E \rightarrow {}^4A_2$ transitions. However, lithium niobate is very often grown as congruent crystals with large lithium deficiency (up to 6% of Li). Therefore, congruent crystals contain many intrinsic defects. This causes large inhomogeneous broadening of sharp R lines, which makes their interpretation more difficult. In addition, some Cr^{3+} centers in $LiNbO_3$ crystals exhibit only broadband luminescence. In this case, identification of their nature is even more difficult. Although several sophisticated techniques have been used to resolve that problem, it still remains unsolved. There is a common agreement that in the congruent crystals doped with relatively low concentration of Cr^{3+} ions or/and codoped with Mg with concentration below 4.5%, the Cr^{3+} ions occupy mainly Li^+ sites.[2,3] If the concentration of Mg codopant is increased above 4.5% threshold level, an additional Cr^{3+} center appears, which has been identified as chromium ions in Nb^{5+} sites (Cr^{3+}_{Nb}).[4–9]

Recently, stoichiometric lithium niobate crystals have been obtained by several methods. In such crystals, spectral linewidths of sharp optical transitions are much more narrow than in congruent ones due to a reduced number of intrinsic defect. This makes them much better for studying the nature of the various Cr^{3+} centers exhibiting much smaller inhomogeneous broadening of the optical transitions, although also an appearance of a few new Cr^{3+} centers has been reported in some stoichiometric crystals.[10–12]

Recently, we have used a diamond-anvil cell high-pressure technique at low temperatures to study the pressure dependence of the luminescence spectra and the luminescence decay times of Cr^{3+} ions in congruent $LiNbO_3$:Cr,MgO crystals.[13] Application of high pressure reduces the distances between a dopant ion and the ligands. Thus it increases the strength of the crystal field experienced by the dopant centers, allowing us to obtain information about their electronic structure. It is especially useful for the identification of the energy structure of Cr^{3+} ions in lithium

niobate crystals since the low-strength crystal field of the Cr^{3+} ions is transformed under the influence of pressure into the high-strength crystal field in which the first excited state of this ion is the ^2E state. This way, instead of broadband luminescence associated with the $^4T_2 \rightarrow {}^4A_2$ transitions, the sharp R lines related to $^2E \rightarrow {}^4A_2$ transitions are observed. This reduces difficulties in the interpretation of the spectra. Using this technique, we were able to show that in the congruent $LiNbO_3$ crystals there is one dominating Cr^{3+} center, denoted as center γ,[14] which corresponds to, most probably, unperturbed Cr^{3+} ions in Li^+ sites. The Cr^{3+} ions in this center experience rather intermediate strength crystal field at ambient pressure, although the $^4T_2$ level is located below the ^2E. The other center present in congruent crystals, denoted as centers β,[14] which exhibit R-line luminescence at ambient pressure, has a slightly stronger crystal field, although again the difference between the energies of the $^4T_2$ and the ^2E levels is negative (or close to 0) at this pressure. The concentration of this center is much smaller than the concentration of the dominating γ center. The remaining low concentration center α (Ref. 14) is a high-strength crystal-field center, i.e., the ^2E state is the lowest excited state of the Cr^{3+} ions in this center at ambient pressure. Most probably, the centers α and β also correspond to the Li^+ site, perhaps perturbed by some kind of intrinsic defect.[14]

In the congruent lithium niobate crystals doped with MgO above a concentration of 4.6%, an additional low-strength crystal-field center exists, denoted as center δ. We could not distinguish the additional R lines associated with this center even at a pressure of about 150 kbar in those crystals.[15] At this pressure, broadband luminescence was still visible in these congruent crystals. The δ center is supposed to correspond to Cr^{3+} ions in the Nb^{5+} site in the $LiNbO_3$ host. Doping the crystals with Mg ions forces the Cr^{3+} ions to occupy this position, which, however, does not occur if the MgO concentration is lower than the 4.6% threshold.

In this paper we report the results of a pressure dependence of Cr^{3+} luminescence of near-stoichiometric $LiNbO_3$ crystals doped with chromium and also codoped with MgO. Codoping with Mg in stoichiometric crystals very efficiently transfers the Cr^{3+} ions into the Nb^{5+} position, and this effect occurs at a much lower concentration of MgO than in congruent crystals.[8,9,16] It is associated with a lower number of Li vacancies in near-stoichiometric crystals, which are supposed to be filled by Mg ions. This way, Cr^{3+} ions are most likely to occupy Nb^{5+} positions. It will be shown that the much smaller inhomogeneous broadening of R lines in the near-stoichiometric crystals allows us to detect the R lines associated with the center δ and establish accurately the strength of the crystal field in this center.

II. EXPERIMENT

The samples used in these studies have been grown by the Czochralski method from a congruent melt to which about 6% of K_2O has been added. This gives rise to a near-stoichiometric crystal with a composition of 49.7 mol. % of Li.[17] Chromium in a concentration of about 0.2 mol. % has been added to the melt. With this melt composition, we grew the crystal for the first sample studied in this paper. A second sample doped with Cr and Mg was cut from a crystal grown from a melt also containing about 1.5% of MgO, although the amount of MgO introduced to the crystals was only equal to 0.2%.

The absorption spectra have been measured in a Hitachi U3501 spectrophotometer. The samples were placed in the closed-cycle cryostat for low-temperature measurements.

Continuous wave emission spectra were obtained using a 514.5-nm line of an argon-ion laser as the excitation source. The spectra were measured with use of a GDM-1000 double grating monochromator equipped with a cooled photomultiplier (EMI 9684B) with an S1-type cathode and an SR530 lock-in amplifier. The spectra were corrected for the quantum efficiency of the photomultiplier. The high-pressure measurements were performed with use of a low-temperature diamond-anvil cell (Diacell Products MCDAC-1). The argon was used as a pressure-transmitting medium. The diamond-anvil cell was mounted into an Oxford 1204 cryostat equipped with a temperature controller for low-temperature measurements. The R_1-line ruby luminescence was used for pressure calibration.[18,19] The polished samples of thickness about 30 μm were loaded into the cell along with a small ruby ball. To measure the luminescence, the argon-ion laser line was focused either on the measured $LiNbO_3$ sample or on ruby. The changes of pressure were done at room temperature in order to minimize nonhydrostatic effects that are known to exist in diamond-anvil cells especially at higher pressure. The hydrostatic conditions could be partially monitored by recording the half-width of the ruby emission. In our measurements we observed an increase of the half-width of ruby luminescence with increasing pressure. The half-width of the R_1 ruby luminescence did not exceed 6 cm^{-1} at high pressures (2.5 cm^{-1} at ambient pressure). This means that the nonhydrostatic effects were rather weak.

The decay kinetics of the luminescence have been measured with use of an SR430 Multichannel Scaler. The large number of decays have been collected in order to obtain good signal-to-noise ratio. The exciting laser beam has been chopped by an acousto-optic modulator with the transient time below 10 ns. The decay kinetics were stored in the computer. The decay times of luminescence were calculated by fitting the decay kinetics with single- or double-exponential curves.

III. EXPERIMENTAL RESULTS AND THEIR INTERPRETATION

A. Absorption and luminescence spectra of bulk $LiNbO_3:Cr^{3+}$ crystals at ambient pressure

The low-temperature absorption spectra of the stoichiometric $LiNbO_3$:Cr (dashed lines) and $LiNbO_3$:MgO,Cr (solid lines) crystals are presented in Fig. 1. The spectra of the crystal doped only with Cr, (dashed line) exhibit strong and sharp R lines. The strongest R lines at 13 770 and 13 808 cm^{-1} are the R_1 and R_2 lines, respectively, associated with the Cr^{3+} center γ. The much weaker sharp line that peaked at 13 680 cm^{-1} is the R_1 line of center β. The R_2 line of this center, which has a peak at 13 744 cm^{-1}, is overlapped with the R_1 line of center γ. No R lines associated with the Cr^{3+} center α are visible in the spectra. In agreement with previously published results, the concentration of center β is much lower than the concentration of Cr^{3+} ions in the domi-

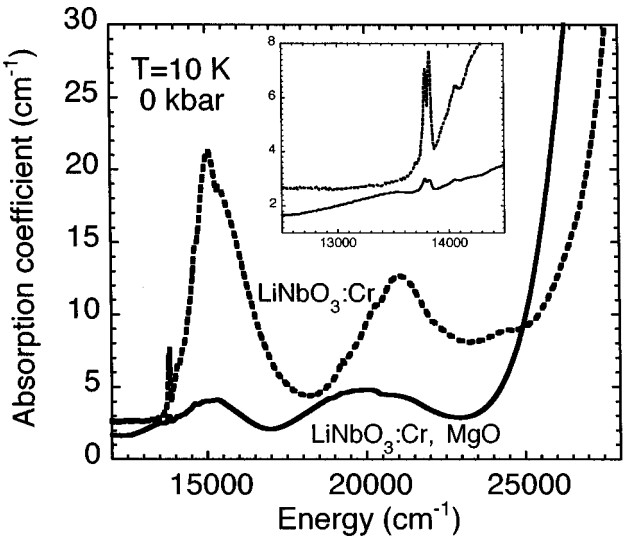

FIG. 1. Absorption spectra of near-stoichiometric $LiNbO_3$:Cr and $LiNbO_3$:CrMgO crystals at temperature $T=10$ K at ambient pressure. In the inset: expanded spectra in the region of the *R* lines.

nating γ center. The full width at half maximum (FWHM) of the *R* lines is about 20 cm^{-1} in our samples, which is about five times less than in the congruent crystals. The broadband structures, which peaked at about 15 000 and 21 000 cm^{-1}, are associated with optical transitions from the ground $^4A_2$ state to the $^4T_2$ and to the $^4T_1$ states, respectively, associated mainly with the Cr^{3+} center γ, as a dominating Cr^{3+} center in this crystal.

The spectra of the $LiNbO_3$:MgO,Cr crystal (solid line) exhibit weaker absorption structures, associated with Cr^{3+} ions, although the initial level of doping in the melt was the same in both crystals. This means that the final concentration of chromium in the γ center introduced to this crystal is much lower than in the case of doping only with Cr. The peak positions of the broadbands in these spectra are shifted towards infrared. This is responsible for the different color of this crystal. The same *R* lines as observed in the crystal doped only with Cr, however with much lower intensity, are visible in the spectra. This means that the absorption spectrum of this crystal is a sum of the absorption associated with the γ center and with an additional center, denoted as center δ, observed in the crystals doped with MgO at the proper level.

Low-temperature luminescence spectra of large crystals at ambient pressure, presented in Fig. 2, exhibit mainly broadband luminescence. Only very weak *R*-line luminescence (presented in the inset in Fig. 2), associated with the so-called center β at 13 680 cm^{-1} and with the center α at 13 605 cm^{-1}, can be observed. The additional line visible at 13 528 cm^{-1} is a zero-phonon line of the $^4T_2 \rightarrow {}^4A_2$ transitions, which is associated with the γ center, dominating in the crystals doped only with chromium. This conclusion is supported by the measurements of the luminescence decay kinetics of this line, which is equal to 9.4 μs and is equal to the decay time of the broadband luminescence. In contrast to that, the luminescence decay times of the α and β centers at ambient pressure are equal to 260 and 240 μs, respectively.

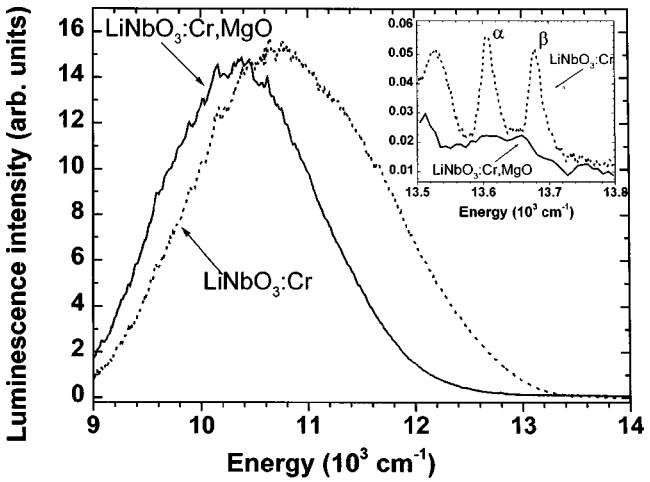

FIG. 2. Luminescence spectra of bulk near-stoichiometric $LiNbO_3$:Cr and $LiNbO_3$:CrMgO crystals at temperature $T=10$ K at ambient pressure, excited by the 514.5-nm argon-ion laser line. In the inset: expanded spectra in the region of the *R* lines.

B. Pressure dependence of luminescence spectra at low temperature

No sharp *R*-line luminescence has been observed in the spectra of examined samples measured with use of the diamond-anvil cell (DAC) at ambient pressure. This is associated with very low luminescence intensity of the α and β centers at this pressure. This behavior is well known to occur in the stoichiometric crystals.[7] Therefore, these centers can be observed only using much larger samples than is possible to load into DAC. However, application of pressure changes profoundly the luminescence spectra of both crystals. The examples of the spectra of the $LiNbO_3$:Cr (green crystal) at a temperature of 10 K are presented in Figs. 3 and 4. At a pressure of about 6 kbar the R_1 line of the β center became clearly visible since the increase of pressure increases the energy of the $^4T_2$ level and the ^2E level became the first excited state of Cr^{3+} ions occupying this center. At higher pressures, beginning from 14 kbar, the R_1 line of the γ centers is visible. A further increase of pressure makes this line the dominating feature in the luminescence spectra of the $LiNbO_3$:Cr near-stoichiometric crystal. The increase of the $R_1(\gamma)$ line intensity proceeds at the expense of the broadband luminescence, associated with the $^4T_2 \rightarrow {}^4A_2$ transitions of the Cr^{3+} ions in the γ center. The broadband luminescence practically disappears at a pressure of about 20 kbar.

The pressure dependence of the luminescence spectra of the stoichiometric $LiNbO_3$:Cr crystal resembles very much this dependence for the congruent one. The main difference is associated with much larger inhomogeneous broadening of the optical transitions in the congruent samples. Due to larger disorder of congruent crystals, the Cr ions in different sites experience a much broader spectrum of strength of the crystal field. Therefore, in congruent crystals the R_1 line associated with the β center is easily visible at ambient pressure even in small crystals loaded into DAC, and the broadband luminescence disappears at slightly higher pressures than in near-stoichiometric ones. In addition to that, we do not observe any additional chromium centers in the luminescence of our near-stoichiometric sample as compared with the congruent sample at any pressure. Figures 3 and 4 docu-

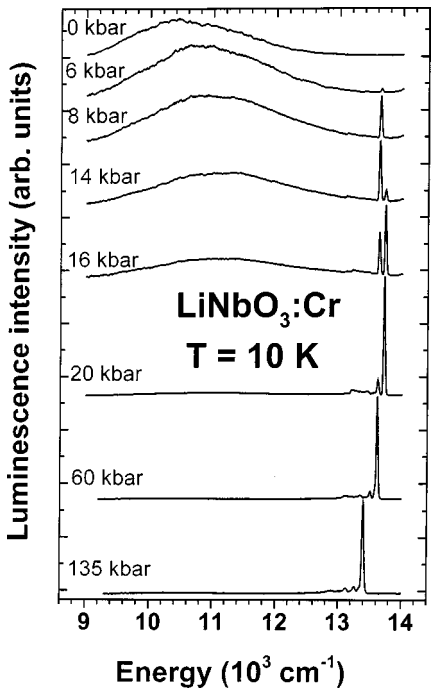

FIG. 3. The pressure dependence of the Cr^{3+} luminescence in near-stoichiometric $LiNbO_3$:Cr(0.1%) crystal at temperature $T = 10$ K.

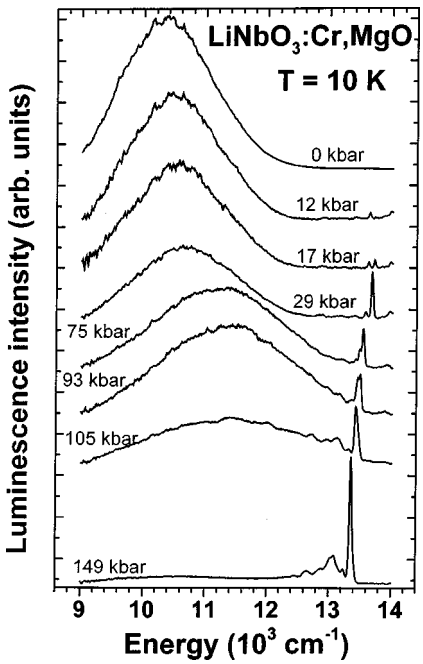

FIG. 5. The pressure dependence of the Cr^{3+} luminescence in near-stoichiometric $LiNbO_3$:Cr MgO crystal at temperature $T = 10$ K.

ment these conclusions and therefore we decided to include them in this paper, although they resemble somehow the data previously published by us.[13]

The pressure dependence of the luminescence spectra of the near-stoichiometric $LiNbO_3$:MgO,Cr crystal (the pink one) is shown in Figs. 5 and 6. At low pressures up to 70 kbar, the luminescence behavior of this sample in the region of the R lines is very similar to the pressure dependence of the luminescence of the crystal doped only with Cr. However, the $LiNbO_3$:MgO,Cr crystal exhibits an additional broadband luminescence, which is not present in the luminescence spectra of the former one at a pressure above 20 kbar. At a pressure larger than 70 kbar, the additional sharp line becomes discernible in the spectra in between the R_1 lines associated with the β and the γ centers. With a further

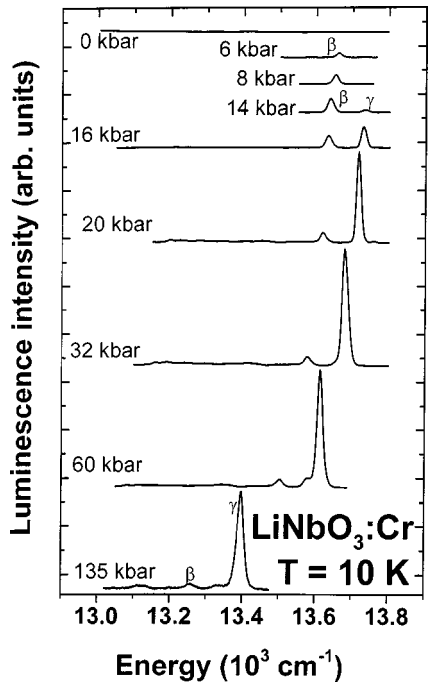

FIG. 4. The pressure dependence of the Cr^{3+} luminescence in near-stoichiometric $LiNbO_3$:Cr(0.1%) crystal at temperature $T = 10$ K in the region of the R lines.

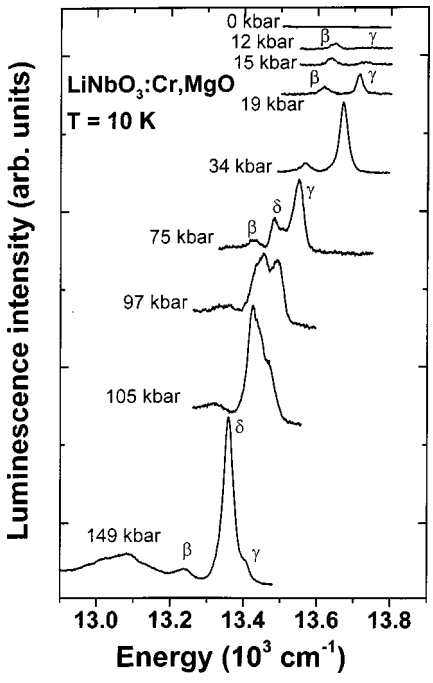

FIG. 6. The pressure dependence of the Cr^{3+} luminescence in near-stoichiometric $LiNbO_3$:CrMgO crystal at temperature $T = 10$ K in the region of the R lines.

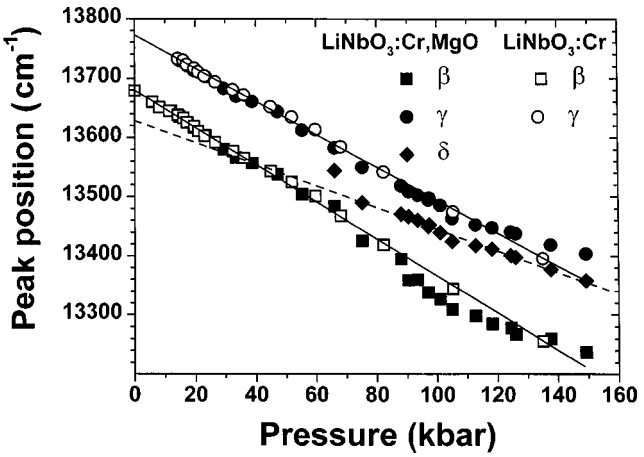

FIG. 7. Spectral positions of the R_1 lines of the β, γ, and δ centers of Cr^{3+} luminescence of near-stoichiometric $LiNbO_3$:Cr and $LiNbO_3$:CrMgO crystals at temperature $T=10$ K as a function of pressure.

increase of pressure, the intensity of this line increases at the expense of the broadband luminescence. At a pressure of about 150 kbar, this line dominates the spectrum and only traces of the broadband luminescence are discernible in the spectra.

We associate this sharp line with the R_1 line of the additional low crystal field δ center, which corresponds to Cr^{3+} ions in Nb^{5+} sites. Here is the important difference between the luminescence of the Cr dopant in congruent and stoichiometric crystals. Due to the large FWHM of the R lines in the congruent samples, we were not able to distinguish the R line associated with the field δ center from the closely located R line associated with the center γ. In addition, the large inhomogeneous broadening means that the broadband luminescence associated with the $^4T_2 \rightarrow {}^2E$ transitions of the Cr^{3+} ions in the δ center does not disappear at a pressure of about 150 kbar, which we applied to the congruent crystal.[15]

The pressure dependence of the positions of the R lines for both examined samples is shown in Fig. 7. The dependence is linear for any center in the examined range of pressures. The pressure coefficients of the position of the R_1 lines of the β and γ centers are similar and equal to -3.2 and -2.9 cm^{-1}/kbar, respectively. The interception points with the energy axis (at ambient pressure) are equal to $(13\,681 \pm 4)$ and $(13\,770 \pm 2)$ cm^{-1} for the β and γ centers, respectively. This agrees very well with the position of the R_1 line for the center β at ambient pressure.

The peak position of the broadband luminescence also depends on pressure and its pressure coefficient is equal to about $+13.5$ cm^{-1}/kbar in the Cr-only-doped sample and to about $+11$ cm^{-1}/kbar in MgO, Cr-doped crystal.

The pressure coefficients of the R-line luminescence of centers β and γ and also the broadband luminescence are practically equal in the stoichiometric and the congruent crystals.

The energy difference at ambient pressure between the positions of the $^4T_2$ and the ^2E states of the Cr^{3+} ions in the γ centers, calculated from the peak energy of the luminescence line associated with the zero-phonon $^4T_2 \rightarrow {}^4A_2$ transitions ($13\,528$ cm^{-1}), observed in the bulk samples and the interception point with the energy axis of the pressure dependence of the position of the R_1 line for this center, is equal to $\Delta_\gamma = -242$ cm^{-1}. This value agrees very well with the value of Δ_γ calculated from the combined effect of the observed redshift of the R lines and the blueshift of the $^4T_2$ band for the γ center, equal to about 16 cm^{-1}/kbar, since the $R_1(\gamma)$ line becomes visible in the luminescence spectra at a pressure of about 14 kbar.

The R_1 line of center β became clearly visible in the spectra at very low pressures. This means that the energy difference at ambient pressure between the positions of the $^4T_2$ and the ^2E levels of the Cr^{3+} ions in the β centers is probably also negative, but rather very small, i.e., these levels are closely located.

The pressure coefficient for the δ center differs considerably from the previous ones and is equal to about -1.8 cm^{-1}/kbar. The interception point with the energy axis is equal to $(13\,628 \pm 6)$ cm^{-1}.

The energy difference at ambient pressure between the positions of the $^4T_2$ and the ^2E states of the Cr^{3+} ions in the δ centers, calculated from the combined effect of the observed redshift of the $R_1(\delta)$ line and the blueshift of the $^4T_2$ band for the δ center, equal to about 13 cm^{-1}/kbar, is equal to at least $\Delta_\delta = -1000$ cm^{-1}, since the $R_1(\delta)$ line became visible in the luminescence spectra at a pressure of about 75 kbar. The true value of Δ_δ can be even larger since the inhomogeneous broadening tends to reduce it.

C. Temperature dependence of the δ-center luminescence

Our measurements have been performed mostly at a low temperature of about 10 K. As a result, only lower-energy R_1 lines of the $^2E \rightarrow {}^4T_2$ luminescence has been observed in the measured spectra. This allows us to resolve more easily the complicated spectra at higher pressures. The splittings of the ^2E level for the α, β, and γ centers (the R_2 lines) have been previously measured in the absorption, luminescence excitation, and emission measurements.[14] In order to obtain information on the splitting of the ^2E level for the δ center, the temperature dependence of this center luminescence has been measured in the sample doped with MgO, in which the δ center occurs, at a pressure of 125 kbar. During these measurements, the spectra of our sample were measured at each temperature together with the spectra of ruby in order to monitor possible changes of pressure by temperature elevation. No changes of position of the R_1 ruby line were observed in the whole temperature range of measurements. We expect that in this temperature range (10–60 K) the temperature shift of the R_1 ruby emission should be below 0.1 cm^{-1} (Ref. 20) (as compared with the pressure shift equal to 0.753 cm^{-1}/kbar). This means that the pressure was kept unchanged during these measurements.

The results are presented in Fig. 8. At temperature $T=10$ K, the R-line luminescence is a convolution of the $R_1(\delta)$, $R_2(\delta)$, and $R_1(\gamma)$ lines. Their positions are marked in Fig. 8. The $R_1(\delta)$ line is dominating at this temperature. At elevated temperatures above 30 K, the $R_2(\delta)$ line became visible at a higher energy of about 17 cm^{-1} than the energy of the $R_1(\delta)$ line. Intensity of the $R_2(\delta)$ line increases with the increase of temperature, which is visible in Fig. 8.

Decay times of both the $R_1(\delta)$ and the $R_2(\delta)$ line are the same at any temperature of measurements. This also con-

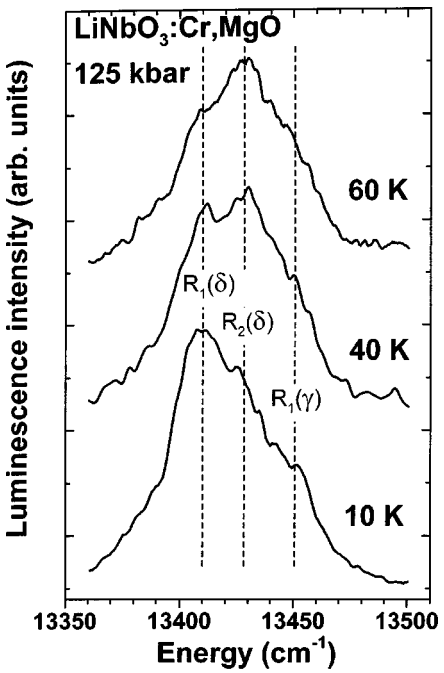

FIG. 8. The temperature dependence of the *R*-line luminescence of center δ at a pressure of 125 kbar.

firms that this additional line that is resolved at elevated temperatures is the R_2 line of center δ, although due to a considerable overlap of the emission of center δ with the luminescence of center γ, we could not fully resolve the lines in order to extract the activation energy of the temperature dependence of the intensity changes of the $R(\delta)$ lines.

The splitting of the ^2E level of the δ center, equal to 17 cm^{-1}, is the lowest among the Cr^{3+} centers occurring in $LiNbO_3$ crystals. It is in the range of the inhomogeneous broadening of the *R* lines in these near-stoichiometric crystals. This is the reason that this splitting cannot be resolved in the congruent crystals.

D. Pressure dependence of the decay kinetics of luminescence

1. Experimental results

The decay kinetics of the broadband and sharp *R*-line luminescence have been measured at temperature $T=10$ K for both types of near-stoichiometric $LiNbO_3$ crystals, doped only with chromium and codoped with magnesium. The pressure dependence of the decay times of the luminescence is presented in Fig. 9. The decay time of the broadband $^4T_2 \rightarrow {}^4A_2$ luminescence in the crystal doped only with Cr is equal to about 9.4 μs in the range of measured pressure. This luminescence, which is associated mainly with the dominating γ center, can be observed only up to 38 kbar. Above that pressure, this luminescence became unmeasurable due to its low intensity.

The broadband luminescence in the crystals doped with Mg is, in contrast, associated mainly with the $^4T_2 \rightarrow {}^4A_2$ of the δ center. The decay time of this luminescence is equal to about 17.6 μs, independent of pressure.

The decay times of the *R*-line luminescence increase with an increase of pressure. The pressure dependences of the *R*-line luminescence decays for the centers β and γ are practically the same in both examined crystals. The decay times change from about 200 μs at low pressures up to about 1.5 ms at a pressure of about 140 kbar. The decay times of the *R*-line luminescence associated with center δ, observed in the crystal codoped with magnesium, change from about 200 μs at a pressure of 105 kbar up to 400 μs at 150 kbar.

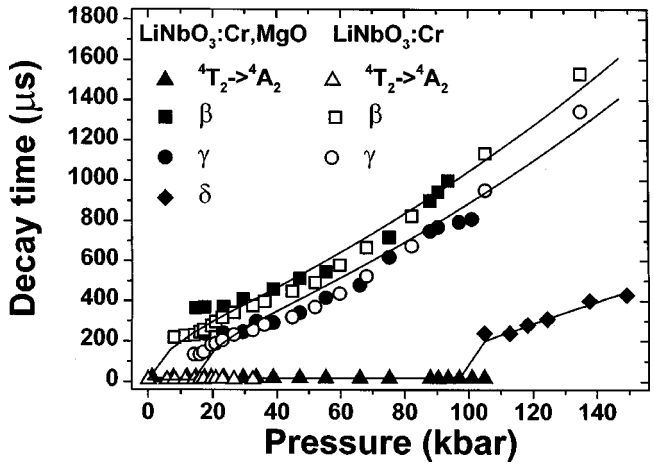

FIG. 9. Pressure dependence of the luminescence decay times of different Cr centers at $T=10$ K. The lines are the computer fits to the experimental data.

2. Theoretical analysis of the emission spectra and luminescence decay times

The pressure dependence of the luminescence decay kinetics and the emission line shapes can be modeled by considering the energetic structure of the Cr^{3+} ion, which consists of $\Gamma_8(^4A_2)$ ground and the $\Gamma_8(^4T_2)$, $\Gamma_8'(^4T_2)$, $\Gamma_7(^4T_2)$, $\Gamma_6(^4T_2)$, $\Gamma_8(^2E)$, $\Gamma_8(^2T_1)$, and $\Gamma_6(^2T_1)$ excited electronic manifolds mixed by the spin-orbit interaction.[21,22] Since the $\Gamma_8(^4A_2)$ ground state is well energetically separated, we have omitted its coupling with the excited states.

We have considered the total Hamiltonian of the system given as a sum of the electronic Hamiltonian, H_e, lattice Hamiltonian, H_l, and electron-lattice interaction Hamiltonian $H_{e\text{-}l}$,

$$H(q,Q)=H_e(q)+H_l(Q)+H_{e-1}(q,Q). \tag{1}$$

Here q and Q are the electronic and configuration coordinate, respectively. The details of this Hamiltonian for the case of Cr^{3+} and equivalent systems are discussed elsewhere.[22–24]

For the purpose of this paper, we have solved the problem using the diabatic representation,[25,26] where the electronic parts of the wave functions have been assumed to be independent of ionic positions. Thus the following Born-Oppenheimer functions represent the diabatic basis:

$$\psi_\Gamma^n(q,Q,s)=\varphi_\Gamma(q,s)\chi_\Gamma^n(q), \tag{2}$$

where $\varphi_\Gamma(q,s)$ and $\chi_\Gamma^n(Q)$ are the electronic and ionic parts of the wave functions, respectively, and ''*s*'' represents the spin, that is, $\frac{1}{2}$ or $\frac{3}{2}$ for doublets and quartets, respectively. According to the above assumptions, the electronic part of the Hamiltonian is the strong crystal-field Hamiltonian. Assuming the octahedral symmetry of the Cr^{3+} site, Γ corre-

TABLE I. Spin-orbit matrix elements (in ξ units).

$H_{\text{s-o}}(\xi)$	$\Gamma_8(^4T_2)$	$\Gamma_8'(^4T_2)$	$\Gamma_8(^2E)$	$\Gamma_8(^2T_1)$	$\Gamma_6(^4T_2)$	$\Gamma_6(^2T_1)$	$\Gamma_7(^4T_2)$
$\Gamma_8(^4T_2)$	$-\frac{1}{6}$	0			0	0	0
$\Gamma_8'(^4T_2)$		$\frac{1}{4}$			0	0	0
$\Gamma_8(^2E)$			0	0	0	0	0
$\Gamma_8(^2T_1)$				0	0	0	0
$\Gamma_6(^4T_2)$					$\frac{1}{4}$		0
$\Gamma_6(^2T_1)$						0	0
$\Gamma_7(^4T_2)$							$-\frac{5}{12}$

sponds to the irreducible representations of the double point group O_h, listed above. The vibronic part of the Hamiltonian describes the vibrations of the ligands. Although we have found that the ion motion is confined,[27] we have used the harmonic approximation for consideration of the vibronic states related to each electronic manifold. This has been done for convenience since in the harmonic approximation the vibronic overlap integrals can be easy calculated by Manneback recurrence formulas.[28]

We have considered the coupling only to the full symmetrical breathing mode. Thus in the harmonic approximation the electronic energies, parametrically dependent on ionic positions and the lattice vibration potentials, are given by the following parabolas:

$$\varepsilon_\Gamma(Q)=\varepsilon_\Gamma^0+S_\Gamma\hbar\omega+\hbar\omega\frac{Q^2}{2}+\sqrt{2S_\Gamma}\hbar\omega Q, \tag{3}$$

where S_Γ is the Huang-Rhys parameter of state Γ. S_Γ is assumed to be zero for all states belonging to the ground electronic configuration, t^3 (all components of the $^4A_2$, ^2E, and $^2T_1$ electronic manifolds).

To calculate the energetic structure of the system, we have taken into account 50 vibronic states related to each electronic manifold. In such a way, we have created the Hamiltonian where the diagonal matrix elements were defined by

$$H_{\Gamma\Gamma}^{nn}=\varepsilon_\Gamma^0+H_{\text{s-o}}^{\Gamma\Gamma}+(n+\tfrac{1}{2})\hbar\omega, \tag{4}$$

where $H_{\text{s-o}}^{\Gamma\Gamma}$ are the spin-orbit matrix elements. The spin-orbit interaction is taken into account by the diagonal as well as by the off-diagonal part of the Hamiltonian. Actually in the diabatic representation, the off-diagonal part of the Hamiltonian is given only by the spin-orbit interaction. Considering the lattice vibrations and electron-lattice coupling, one obtains that the spin-orbit interaction is moderated by the vibronic overlap integrals. Thus the off-diagonal part of the Hamiltonian is given by

$$H_{\Gamma\Gamma}^{nm}=H_{\text{s-o}}^{\Gamma\Gamma'}\int\chi_\Gamma^{n*}(Q)\chi_{\Gamma'}^{m}(Q)dQ. \tag{5}$$

The spin-orbit matrix elements, $H_{\text{s-o}}^{\Gamma\Gamma'}$, are listed in Table I. The vibronic structure of the excited states that resulted from the diagonal part of the Hamiltonian (see Ref. 28) is presented in Fig. 10(a). In Fig. 10(b), the spin-orbit interaction that is yielded from the off-diagonal part of the Hamiltonian is indicated.

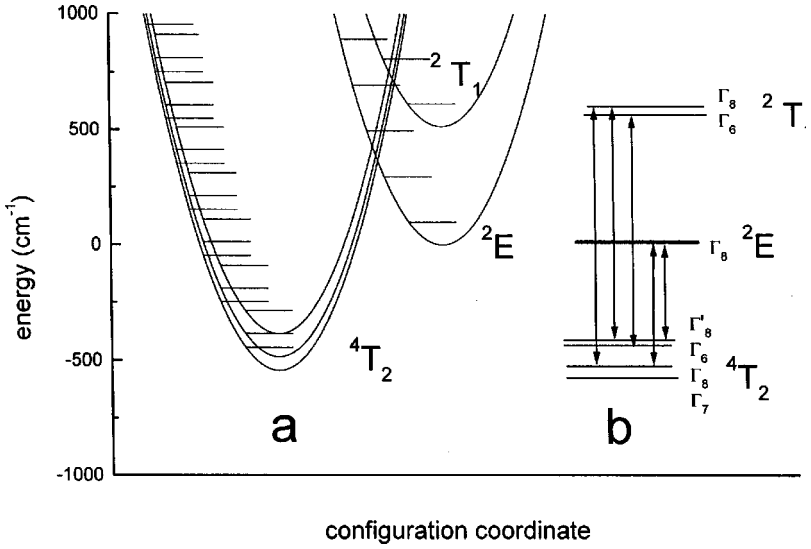

FIG. 10. (a) The adiabatic energies of the system represented by the diagonal part of the diabatic Hamiltonian [Eq. (4)]. One can see that the Γ_8' and Γ_6 components of the $^4T_2$ state as well as $\Gamma_8\Gamma_6$ components of the $^2T_1$ state are degenerated. This degeneration is removed by the off-diagonal part of the Hamiltonian [Eq. (5)]. (b) The off-diagonal part of the spin-orbit interaction, see also Table I. Energies are given with respect to the minimum energy of the ^2E electronic manifold.

Diagonalization of the Hamiltonian given by Eqs. (4) and (5) allows us to calculate the vibronic energies as well as the wave functions of the system. The resulting states are characterized only by the single quantum number k, which is related to the energy E^k. The respective wave function is a mixture of all considered states and is given by the following superposition:

$$\Phi^k(q,Q)=\sum_{jm} a_j^{km}(\tfrac{1}{2})\varphi_j(q,\tfrac{1}{2})\chi_j^m(Q) + \sum_{in} a_i^{kn}(\tfrac{3}{2})\varphi_i(q,\tfrac{3}{2})\chi_i^n(Q). \quad (6)$$

Here the first and the second sum represent the doublet and quartet contributions; $a_i^{kn}(\frac{3}{2}), a_j^{km}(\frac{1}{2})$ are coefficients obtained in the framework of the diagonalization procedure. Since the ground electronic manifold is the $^4A_2$ quartet, only the transitions from the quartet excited states contribute to the luminescence. One calculates the contribution related to the transition from the $\Phi^k(q,Q)$ state to the lth vibronic state of the ground electronic manifold $^4A_2$ as follows:

$$I_{kl}=\sum_i \left| \int \left(\varphi_{^4A_2}(q,\tfrac{3}{2})M(q)\varphi_i^*(q,\tfrac{3}{2})dq \times \sum_n a_i^{kn}(\tfrac{3}{2}) \int (\chi^l_{^4A_2})(Q)(\chi_i^n)^*(Q)dQ \right|^2 n_i, \quad (7)$$

where n_i is the degeneration of the states, which is 4 for Γ_8 and Γ_8', and 2 for Γ_6 and Γ_7.

Quantity $\varphi_{^4A_2}(q,\frac{3}{2})M(q)\varphi_i^*(q,\frac{3}{2})dq$ is the electronic transition moment. Since we have not considered a polarization, we have assumed that this quantity is the same for all quartet components. In such a way, the intensity of the transitions between the kth excited state and the lth vibronic state of the ground electronic manifold is proportional to the following sum of the vibronic overlap integrals:

$$I_{kl}\propto \sum_i \sum_n \left| a_i^{kn}(\tfrac{3}{2}) \int (\chi^l_{^4A_2})(Q)(\chi_i^n)^*(Q)dQ \right|^2 n_i. \quad (8)$$

Using our model, one can reproduce the emission line shape considering the energetic structure of a particular Cr^{3+} site. For given temperature one obtains

$$I(\hbar\Omega,T)=\sum_k \sum_l I_{kl}(E_{^4T_2},E_{^2E}) \times \delta\{\hbar\Omega-[E^k-(E^I_{^4A_2})]\}S[(E^k-E^0)/kT]. \quad (9)$$

In Eq. (9) it is indicated explicitly that the emission is related to the Cr^{3+} site characterized by specific energies of the $^4T_2$ and ^2E states. The intensity $I_{kl}(E_{^4T_2},E_{^2E})$ is expressed by Eq. (8). Specific energies of the $^4T_2$ and ^2E electronic manifolds are the input parameters of the total Hamiltonian (4). $S[(E^k-E^0)/kT]$ is the Boltzmann occupation factor and E^0 is the lowest energy of the excited electronic manifold.

One can calculate the luminescence decay time, τ. Considering that the luminescence lifetime is related to the radiative transition probability, P, by the relation $\tau=P^{-1}$ and the radiative transition probability is proportional to the emission intensity, one obtains

$$\tau^{-1}(E_{^4T_2},E_{^2E},T)=\frac{1}{\tau_0}\sum_k \sum_l I_{kl}(E_{^4T_2},E_{^2E}) \times S[(E^k-E^0)/kT], \quad (10)$$

where $I_{kl}(E_{^4T_2},E_{^2E})$ is given by Eq. (8). τ_0 is the time constant that represents the pure quartet lifetime and is related to the transition moment as follows:

$$\tau_0^{-1}=\left| \int (\varphi^*_{^4A_2})(q,\tfrac{3}{2})M(q)(\varphi_{^4T_2})(q,\tfrac{3}{2})dq \right|^2. \quad (11)$$

Actually τ_0 was taken as the luminescence decay time of the broadband $^4T_2\rightarrow{}^4A_2$ luminescence measured at $T=10$ K. Equations (9) and (10) result in a dependence of the luminescence line shape as well as the luminescence decay time on the energetic structure of a chromium ion.

One can see that energies of the $^4T_2$ and ^2E electronic manifolds depend linearly on pressure. Thus one describes the response of the system on pressure using the following two parameters: the pressure coefficients $dE(^4T_2)/dp = 10[d(Dq)/dp]$ and $dE(^2E)/dp$ for the energies of the $^4T_2$ and ^2E states, respectively.

The experimental pressure dependences of the luminescence decay times have been approximated with formula (10). The calculations were performed in the following way. First, the decay times of the luminescence for center γ were fitted with Eq. (10). The values of the spin-orbit interaction, the electron-lattice coupling energy, and the phonon energy were used as adjustable parameters. The value of the energy difference between the $^4T_2$ and the ^2E levels ($\Delta_\gamma = -242\ \mathrm{cm}^{-1}$) is known for this center from the luminescence data. We have assumed that the spin-orbit interaction, electron-lattice coupling energy, and phonon energy do not depend on pressure. Subsequently, the pressure dependence of the luminescence decay time of $R_1(\beta)$ was fitted with formula (10), using the values of the spin-orbit interaction and the electron-lattice coupling energy obtained from the previous fit. This time only the value of the energy difference between the $^4T_2$ and the ^2E levels (Δ_β) was treated as an adjustable parameter. The value of the Δ_β obtained from the fit is equal to $\Delta_\beta=-20\ \mathrm{cm}^{-1}$. The results of the fits are presented in Fig. 9. We consider the quality of the fits as very good. The small deviations observed at lower pressures can be associated with the assumption of pressure-independent values of the spin-orbit interaction, electron-lattice coupling, and phonon energies. These values depend on the pressure,[29] although this dependence is rather weak. The values of the parameters obtained from the computer fits and used for the fits are listed in Table II.

The parameters obtained from the fit of Eq. (10) to the experimental results of the luminescence decay kinetics of the center δ differ considerably from those obtained from the fits to the data for centers β and γ. It was impossible to obtain a good fit to this dependence using the values of the spin-orbit interaction, electron-lattice coupling, and phonon

TABLE II. Parameters of the Cr^{3+} sites in $LiNbO_3$. The values of the energy levels $^4T_2$, ^2E, and Δ are given for ambient pressure at temperature $T=10$ K.

Cr^{3+} site	Site identification	$E(^4T_2)$ (cm^{-1})	$dE(^4T_2)/dp$ (cm^{-1}/kbar)	$E(^2E)$ R_1 line (cm^{-1})	^2E splitting (cm^{-1})	$dE(^2E)/dp$ (cm^{-1}/kbar)	$\Delta=E(^4T_2)-E(^2E)$ (cm^{-1})	Spin-orbit parameter ξ (cm^{-1})	$Sh\omega$ (cm^{-1})	$h\omega$ (cm^{-1})
α	Li^+ distorted			13 608	95[a]		>0			
β	Li^+ distorted		13.5	13 681±4	64[a,b]	−3.2	−20	290	2100	350
γ	Li^+	10 850	13.5	13 770±2	38[a,b]	−2.9	−242	290	2100	350
δ	Nb^{5+}	10 370	11	13 628±6	17[b]	−1.8	<−1270	400	1995	230

[a]P. I. Macfarlane, K. Holliday, J. F. H. Nicholls, and B. Henderson, J. Phys.: Condens. Matter **7**, 9643 (1995).
[b]This work.

energies obtained from the fits to the data for center β and γ. The values of the pressure coefficients of the R_1-line and the broadband luminescence are also different. The good fit was obtained using the values of the spin-orbit parameter, electron-lattice coupling, and phonon energies equal to 400, 1995, and 230 cm^{-1}, respectively. Although these values are quite different from those obtained for centers β and γ, it is not surprising, since the center δ has quite a different nature from the former ones.

The value of the Δ_δ energy difference, obtained from the fit, is equal to $\Delta_\beta=-1270\,cm^{-1}$. We consider this value as consistent with that estimated from the total pressure shifts of the $^4T_2$ and ^2E levels for the δ center, since the inhomogeneous broadening can influence the former estimation, making this value smaller.

IV. CONCLUSIONS

Near-stoichiometric $LiNbO_3$ crystals have several advantages over the congruent ones. The most important property of those crystals for our studies is the much smaller number of native defects that results in a several times smaller linewidth of the electronic transitions of the dopants, observed in these crystals. Several Cr^{3+} centers have been detected in lithium niobate crystals, and also some additional centers have been observed in the stoichiometric ones.[1,30–34] Although our studies show that the dominating Cr^{3+} centers in congruent and near-stoichiometric $LiNbO_3$ crystals are practically the same, the smaller linewidth of the electronic transitions of the Cr dopant in the stoichiometric crystals allowed us to perform the high-pressure luminescence studies on this system with much better resolution. Thus it was possible to obtain the information on the energy structure of various Cr^{3+} centers in $LiNbO_3$:Cr with much better accuracy than in congruent samples. It turned out to be particularly important for the studies of the δ center, which occurs in the $LiNbO_3$:MgO,Cr. In such near-stoichiometric crystals, the δ center is a dominating one. Thus the absorption spectrum of such crystals is practically associated with the δ center. A much better resolution of measurements allowed us to obtain the value of the splitting of the ^2E level for this center. It is equal to 17 cm^{-1} and it is the smallest among various Cr^{3+} centers in $LiNbO_3$. The values of the ^2E level splitting for different chromium centers in $LiNbO_3$ are also listed in Table II.

The δ center corresponds to the Cr^{3+} ions in the Nb^{5+} sites in $LiNbO_3$ crystals. The EPR data show that this center is almost isotropic. The very small value of the ^2E level splitting of these centers confirms the EPR results, i.e., it is in very good agreement with the almost octahedral symmetry of this center. The ^2E level splitting occurs due to distortion from the ideal octahedral symmetry[33] and, for example, does not exist in perfectly octahedral sites in MgO:Cr crystal. The much larger intensity of the phonon replicas observed for the δ center at the highest pressure than for the γ (Cr^{3+}_{Li}) center also shows that the oxygen octahedron of the δ center is much less distorted than that of the γ center, which is in agreement with our model, which considers only coupling with fully symmetrical breathing modes. In undoped $LiNbO_3$ crystals, both Li^+ and Nb^{5+} sites have C_3 symmetry. Apparently a large lattice relaxation occurs in the Nb^{5+} site when the Cr^{3+} ion substitutes the Nb^{5+} ion and somehow the lowest energy is achieved in near-octahedral symmetry. This does not occur when chromium ions occupy Li^+ sites. Nevertheless, a small value of the ^2E splitting for the δ center exists and this shows that the symmetry of this site is not perfectly octahedral.

Knowing the value of the absorption peaks associated with $^4A_2\rightarrow{}^4T_2$ and $^4A_2\rightarrow{}^4T_1$ transitions and extrapolated position of the ^2E level at ambient pressure, it is possible to estimate the values of the crystal-field Racah parameters for the δ center at ambient pressure, using a procedure described, for example, in Ref. 34. The values of those parameters are equal to $Dq=1440\,cm^{-1}$, $B=505\,cm^{-1}$, and $C=3266\,cm^{-1}$.

The experimental pressure dependences of the decay times of different Cr^{3+} centers are well described by the presented theory. The values of the energy difference between the $^4T_2$ and the ^2E excited levels, Δ, estimated from the computer fits of the theory and from the observed pressure shifts of the appropriate levels for β, γ, and δ centers are consistent with each other. The Δ_γ value for center γ, known from the position of the zero-phonon line associated with the $^4T_2\rightarrow{}^4A_2$ transitions, is also consistent with both the computer fit of the pressure dependence of the decay times and the pressure shifts of the $^4T_2$ and the ^2E levels.

ACKNOWLEDGMENTS

A.S. acknowledges financial support from Direccion General de Ensenanza Superior e Investigacion Cientifica of Spain during his sabbatical stay at Universidad Autonoma de Madrid. This work was partially supported by the Polish Committee for Scientific Research Grant No. 2P03B 003 13. The technical help of Dr. J. E. Dmochowski is also acknowledged.

[1] G. Malovichko, V. Grachev, E. Kokanyan, and O. Shirmer, Phys. Rev. B **59**, 9113 (1999), and references therein.
[2] J. Garcia Sole, L. E. Bausa, D. Jaque, E. Montoya, H. Murrieta, and F. Jaque, Spectrochim. Acta A **54**, 1571 (1998).
[3] J. Diaz-Caro, J. Garcia-Sole, J. L. Martinez, B. Henderson, F. Jaque, T. P. J. Han, Opt. Mater. **10**, 69 (1998).
[4] E. Camarillo, J. Tocho, I. Vergara, E. Diegues, J. Garcia Sole, and F. Jaque, Phys. Rev. B **45**, 4600 (1992).
[5] F. Jaque, J. Garcia-Sole, E. Camarillo, F. J. Lopez, H. Murrieta S., and J. Hernandez, Phys. Rev. B **47**, 5432 (1993).
[6] J. Diaz-Caro, J. Garcia-Sole, D. Bravo, J. A. Sanz-Garcia, F. J. Lopez, and F. Jaque, Phys. Rev. B **54**, 13 042 (1996).
[7] F. Lhomme, P. Bourson, M. D. Fontana, G. Malovichko, M. Aillerie, and E. Kokonyan, J. Phys.: Condens. Matter **10**, 1137 (1998).
[8] J. Diaz-Caro, J. Garcia-Sole, J. L. Martinez, B. Henderson, F. Jaque, and T. P. J. Han, Opt. Mater. **10**, 69 (1998).
[9] G. A. Torchia, J. A. Sanz-Garcia, J. Diaz-Caro, F. Jaque, and T. P. J. Han, Chem. Phys. Lett. **288**, 65 (1998).
[10] P. F. Bordui, R. G. Norwood, C. D. Bird, and G. D. Calvert, J. Cryst. Growth **113**, 61 (1991).
[11] K. Kitamura, Y. Furukawa, and N. Iyi, Ferroelectrics **202**, 21 (1997).
[12] G. I. Malovichko, V. G. Grachev, L. P. Yurchenko, V. Ya. Proshko, E. P. Kokanyan, and V. T. Gabrielyan, Phys. Status Solidi A **133**, K29 (1992).
[13] A. Kaminńska, J. E. Dmochowski, A. Suchocki, J. Garcia-Sole, F. Jaque, and L. Arizmendi, Phys. Rev. B **60**, 7707 (1999).
[14] P. I. Macfarlane, K. Holliday, J. F. H. Nicholls, and B. Henderson, J. Phys.: Condens. Matter **7**, 9643 (1995).
[15] A. Kamińska, A. Suchocki, M. Grinberg, J. Garcia-Sole, F. Jaque, and L. Arizmendi, J. Lumin. **87–89**, 571 (2000).
[16] G. A. Torchia, J. A. Sanz-Garcia, F. J. Lopez, D. Barvo, J. Garcia-Sole, F. Jaque, H. G. Gallagher, and T. P. J. Han, J. Phys.: Condens. Matter **10**, L341 (1998).
[17] M. D. Serrano, V. Bermudez, L. Arizmendi, and E. Dieguez, J. Cryst. Growth **210**, 670 (2000).
[18] G. J. Piermarini, S. Block, J. D. Barnett, and R. A. Forman, J. Appl. Phys. **46**, 2774 (1975).
[19] R. A. Noack and W. B. Holzapfel, in *High Pressure Science and Technology*, edited by K. D. Timmerhaus and M. S. Barber (Plenum, New York), Vol. 1, p. 748.
[20] D. E. McCumber and M. D. Sturge, J. Appl. Phys. **34**, 1682 (1963).
[21] B. Henderson and G. F. Imbush, *Optical Spectroscopy of Inorganic Crystals* (Oxford University Press, Oxford, 1989).
[22] M. Grinberg, J. Lumin. **54**, 369 (1993).
[23] Czeslaw Koepke, Krzysztof Wiśniewski, Marek Grinberg, David L. Russell, Keith Holliday, and George H. Beall, J. Lumin. **78**, 135 (1998).
[24] M. Grinberg, A. C. Felici, T. Papa, and M. Piacentini, Phys. Rev. B **60**, 8595 (1999).
[25] F. T. Smith, Phys. Rev. **179**, 111 (1969).
[26] M. Grinberg, A. Mandelis, and K. Fieldsted, Phys. Rev. B **48**, 5935 (1993).
[27] Marek Grinberg, Irena Sokólska, Stefan Kuck, and W. Jaskólski, Phys. Rev. B **60**, 959 (1999).
[28] C. Manneback, Physica (Amsterdam) **11-12**, 1001 (1951).
[29] A. Jayaraman and A. A. Balman, J. Appl. Phys. **60**, 1208 (1986).
[30] S. A. Basun, G. M. Salley, A. A. Kaplyanskii, K. Polgar, H. G. Gallagher, L. Lu, and U. Happek, J. Lumin. **83–84**, 435 (1999).
[31] G. M. Salley, S. A. Basun, G. F. Imbush, A. A. Kaplyanskii, S. Kapphan, R. S. Meltzer, and U. Happek, J. Lumin. **83–84**, 423 (1999).
[32] F. Lhomme, P. Bourson, G. Boulon, Y. Guyot, R. Burlot-Loison, M. D. Fontana, A. Aillerie, and G. Malovichko, J. Lumin **83–84**, 441 (1999).
[33] A. I. Schawlow, A. H. Piksis, and S. Sugano, Phys. Rev. **122**, 1469 (1961).
[34] W. Ryba-Romanowski, S. Golab, G. Dzik-Dominiak, I. Sokólska, and M. Berkowski, J. Alloys Compd. **284**, 22 (1999), and references therein.